Observation of an Efimov-like resonance in ultracold atom-dimer scattering

S. Knoop*,[1] F. Ferlaino,[1] M. Mark,[1] M. Berninger,[1]
H. Schöbel,[1] H.-C. Nägerl,[1] and R. Grimm[1,2]

[1]*Institut für Experimentalphysik und Zentrum für Quantenphysik, Universität Innsbruck, 6020 Innsbruck, Austria*

[2]*Institut für Quantenoptik und Quanteninformation, Österreichische Akademie der Wissenschaften, 6020 Innsbruck, Austria*

**e-mail: steven.knoop@uibk.ac.at*

(Dated: July 21, 2008)

The field of few-body physics has originally been motivated by understanding nuclear matter. New model systems to experimentally explore few-body quantum systems can now be realized in ultracold gases with tunable interactions [1, 2]. Albeit the vastly different energy regimes of ultracold and nuclear matter (peV as compared to MeV), few-body phenomena are universal for near-resonant two-body interactions [2]. Efimov states represent a paradigm for universal three-body states [3], and evidence for their existence has been obtained in measurements of three-body recombination in an ultracold gas of caesium atoms [1]. Interacting samples of halo dimers [4] can provide further information on universal few-body phenomena. Here we study interactions in an optically trapped mixture of such halo dimers with atoms, realized in a caesium gas at nanokelvin temperatures. We observe an atom-dimer scattering resonance, which we interpret as being due to a trimer state hitting the atom-dimer threshold. We discuss the close relation of this observation to Efimov's scenario [3], and in particular to atom-dimer Efimov resonances [5, 6, 7].

Ultracold quantum gases offer an unprecedented level of control and are versatile systems to investigate interacting quantum systems. Their unique property is that the two-body interaction, as described by the s-wave scattering length a, can be magnetically tuned through Feshbach resonances [8, 9, 10]. When $|a|$ is tuned to values much larger than the range of

the two-body potential, one enters the universal regime [2], where details of the short range interaction become irrelevant because of the long-range nature of the wavefunction. For ground state alkali atoms the range of the interaction potential is determined by the van der Waals interaction and is given by $r_{\mathrm{vdW}} = \frac{1}{2}(2\mu C_6/\hbar^2)^{1/4}$, where C_6 is the van der Waals dispersion coefficient and μ is the reduced mass. A manifestation of universality in two-body physics is the existence of a *quantum halo* dimer state at large positive a, for which the binding energy is given by the universal expression $E_{\mathrm{b}} = \hbar^2/(2\mu a^2)$ [11]. In the field of ultracold gases such halo dimers, with $a \gg r_{\mathrm{vdW}}$ and $E_{\mathrm{b}} \ll E_{\mathrm{vdW}} = \hbar^2/(2\mu r_{\mathrm{vdW}}^2)$, can be experimentally realized [4, 12], with the unique possibility to tune the properties of the halo dimers across the universal and non-universal regimes. The concept of universality extends beyond two-body physics to few-body phenomena [2]. So far pure atomic systems have been used to experimentally study universal three-body physics. By introducing halo dimers a new class of phenomena becomes accessible, including universal atom-dimer and dimer-dimer scattering.

Here we focus on three-body systems consisting of three identical bosons. In particular, we consider the situation in which two atoms are bound, forming a halo dimer, and scatter with a third, free atom. The atom-dimer system under investigation consists of ^{133}Cs atoms in their lowest spin state, labeled by the total spin quantum number $F = 3$ and its projection $m_F = 3$. The caesium atoms represent an excellent system to study few-body physics with bosons at large scattering lengths because of their unique scattering properties [13]. The scattering length a at low magnetic fields is shown in the inset of Fig. 1. Its unusual magnetic-field dependence is explained by a broad Feshbach resonance at a magnetic field of -12 G [1, 14] along with an extraordinarily large background scattering length and allows to tune a from large negative to positive values with a zero crossing at 17 G. Note that a negative magnetic field corresponds to a sign reversal of the projection quantum number m_F.

The three-body energy spectrum is shown in Fig. 1, illustrating the energies of trimer states (red dashed curves) and atom-dimer thresholds (blue solid curves). Here zero energy corresponds to three free atoms with zero kinetic energy. The energy of an atom-dimer threshold thus simply corresponds to the binding energy of a dimer. The energy dependencies of these thresholds are well known, because of the precise knowledge the caesium two-body spectrum [13, 15]. The dimer state that corresponds to the atom-dimer threshold at positive

magnetic fields carries halo character as $a \gg r_{\mathrm{vdW}}$ is fulfilled in a wide magnetic-field range; for caesium $r_{\mathrm{vdW}} = 100\,a_0$, where a_0 is Bohr's radius, and $E_{\mathrm{vdW}} = h \times 2.7$ MHz. Below 20 G the dimer state bends downwards into the non-universal region because of an avoided crossing with the dimer state that causes the Feshbach resonance at -12 G.

The trimer states, as illustrated in Fig. 1, are located in the regime where $|a|$ exceeds r_{vdW}, with binding energies well below E_{vdW}. We therefore refer to them as Efimov states [3], although sometimes more strict definitions are used [16]. An Efimov trimer intersects the three-atom threshold, at which three free atoms couple resonantly to a trimer. Similarly, an Efimov trimer couples to a halo dimer and a free atom at the atom-dimer threshold. The energy spectrum of trimer states is not precisely known, but their appearance at the thresholds can give clear signatures of their locations. The observation of a giant three-body recombination loss resonance in an ultracold atomic caesium sample at 7.5 G, corresponding to $a = -850\,a_0$, has pinpointed the location at which one of the Efimov states hits the three-atom threshold [1]; see open arrow. The next Efimov resonance in three-body recombination loss is predicted at negative magnetic fields, in principle accessible with atoms in the $F = 3$, $m_F = -3$ state. Unfortunately, in practice its observation will be obscured by fast two-body losses [17]. Several studies have suggested the intersection of a trimer state with the atom-dimer threshold for positive magnetic fields below 50 G [18, 19, 20]; see filled arrow. The appearance of an Efimov trimer at the atom-dimer threshold is predicted to manifest itself in a resonance in atom-dimer relaxation [6, 7].

Atom-dimer relaxation is energetically possible because of the presence of deeply bound dimer states, providing many inelastic channels for collisions between atoms and weakly bound dimers. This process leads to loss of both the atom and the dimer from the trap, as the acquired kinetic energy is in general much larger than the trap depth. The particle loss is described by the rate equation $\dot{n}_{\mathrm{D}} = \dot{n}_{\mathrm{A}} = -\beta n_{\mathrm{D}} n_{\mathrm{A}}$, where $n_{\mathrm{D}}(n_{\mathrm{A}})$ is the molecular (atomic) density and β denotes the loss rate coefficient for atom-dimer relaxation. In the non-universal regime, relaxation loss in ultracold atom-dimer samples has been studied in various systems [21, 22, 23, 24, 25, 26] and was found to be essentially independent of the magnetic field. In the universal regime, suppression of loss has been observed in systems involving fermions [27, 28].

Starting point of our measurements is an ultracold atom-dimer mixture prepared in a crossed-beam optical dipole trap in the temperature range of 30-250 nK (see Methods sec-

tion). The dimers are created by Feshbach association [12, 29] at a 200-mG wide Feshbach resonance at 48 G (not shown in Fig. 1) and then transferred into the halo dimer state [4, 15]. For our lowest temperatures we obtain a mixture of about 3×10^4 atoms and 4×10^3 dimers. After preparation of the mixture we ramp to a certain magnetic field and wait for a variable storage time. Then we switch off the trap and let the sample expand before ramping back over the 48-G resonance to dissociate the molecules, after which standard absorption imaging is performed. During the expansion a magnetic field gradient is applied to spatially separate the atomic and molecular cloud (Stern-Gerlach separation) [29]. In this way we simultaneously monitor the number of atoms and dimers, see Fig. 2a. A typical loss measurement is shown in Fig. 2b. We observe a fast loss of dimers on the timescale of a few tens of a millisecond. In order to obtain β we have set up a dimer loss model based on the above-mentioned rate equation (see Methods section). Because the number of atoms greatly exceeds the number of dimers, a simple analytic expression can be derived, which is fitted to the data. The loss of dimers due to dimer-dimer relaxation is small and is taken into account; the corresponding loss rate for this process was measured independently using a pure dimer sample [4].

The resulting β is shown in Fig. 3 as a function of the two-body scattering length a, using the magnetic field dependence of the scattering length (inset of Fig. 1); the inset shows the same data as a function of the magnetic field. For $a < 0$ ($B < 17$ G) we observe an essentially constant β of about 1.5×10^{-11} cm^{3}s^{-1}, similar to other observations in the non-universal regime. A constant β can be understood by the fact that in this region the dimers are non-universal and therefore their properties are not directly connected to the scattering length [4, 12]. For $a > 0$ we observe a resonance at about $a = 400\, a_0$ ($B = 25$ G), where β increases by one order of magnitude to 1.5×10^{-10} cm^{3}s^{-1}. Two data sets at different temperatures are shown, namely at 40(10) nK (blue open triangles) and 170(20) nK (red closed squares). Both data sets give the same behaviour regarding resonance position and loss rate, showing that the measurements are in the threshold regime in which the loss rate is independent of the collision energy and not unitarity limited. We interpret the observed resonance as the expected manifestation of a trimer state hitting the atom-dimer threshold.

Even though the position of the resonance is not far in the universal regime, we compare our findings with the prediction from effective field theory in the universal limit [7]. We consider the analytic expression $\beta = C_{\mathrm{AD}}(a)\hbar a/m$ with $C_{\mathrm{AD}}(a) =$

$D\left[\sinh(2\eta_*)/\left(\sin^2\left[s_0\ln(a/a_*)\right]+\sinh^2\eta_*\right)\right]$, where $s_0 = 1.00624$. The logarithmically periodic dependence of $C_{\rm AD}(a)$ on a is characteristic for Efimov physics. Here a_* describes the position at which the Efimov trimer hits the atom-dimer threshold, defined up to a factor $e^{\pi/s_0} \approx 22.7$. The dimensionless quantity η_* is related to the lifetime of Efimov states near threshold, and thus characterizes the width of the resonance. We have fitted the analytic expression to the 170 nK data for $a > r_{\rm vdW} = 100a_0$, with a_*, η_* and D as free parameters. The result is shown as the solid curve in Fig. 3. We find that the analytic expression describes the data well, in particular the asymmetric shape of the resonance is well represented by the universal prediction. For the resonance position and the width parameter we obtain $a_* = 367(13)\,a_0$ and $\eta_* = 0.30(4)$, respectively. Both parameters are free in the framework of Ref. [7]. For D we find 2.0(2), for which Ref. [7] predicts a fixed value of 20.3.

According to the universal theory, observations on atom-dimer relaxation are connected to those in three-body recombination [2]. The three-body recombination loss rate can be expressed as $L_3 = 3C_\pm(a)\hbar a^4/m$, where $C_+(a)$ $(a > 0)$ and $C_-(a)$ $(a < 0)$ are again logarithmically periodic functions of a (see [1] and references herein). From a fit to the three-body recombination data a maximum in $C_+(a)$ was found at $a_+ = 1060(70)\,a_0$ [1]. Universal theory predicts $a_* \approx 1.1a_+$ from which an atom-dimer resonance would be expected around $1,200\,a_0$. We find the resonance at a smaller value of a, implying that here an obvious universal connection is absent. The universal theory also connects Efimov-related features for $a < 0$ and $a > 0$. The three-body recombination resonance at $a_- = -850(20)\,a_0$ would correspond to an atom-dimer resonance around $900\,a_0$, also significantly shifted from our present finding. This may be related to the fact that the transition from $a < 0$ to $a > 0$ takes place via a zero crossing and not via a pole as in the Efimov scenario [1, 30]. A universal connection was suggested by the three-body recombination data [1], but in view of the new observations this might have been fortuitously [30].

The observation of a resonance shows that atom-dimer relaxation measurements can provide information on weakly bound trimer states in a complementary way to three-body atomic recombination. Our observations in three-body systems involving caesium follow qualitatively the Efimov scenario, with a three-body recombination resonance at $a < 0$ and an atom-dimer relaxation resonance at $a > 0$. However, the relation between the different features is quantitatively not well described by the universal theory. A simple explanation might be that a is not large enough for a straight-forward application of predictions valid in

the universal limit. This raises the question whether it is possible to extend universal theory by incorporating non-universal corrections [31] or whether a fully non-universal theory would be required.

Further experiments around Feshbach resonances at higher magnetic fields, in particular around a broad one at 800 G [16], can provide deeper insight into the universal aspects of three-body physics. First of all, in the universal theory the locations of three-body recombination and atom-dimer relaxation features only depend on the scattering length. Under this assumption our observations in the low magnetic field range will reappear at higher magnetic fields at the same values of the scattering length. Secondly, at the Feshbach resonances the regions with $a < 0$ and $a > 0$ are connected via a pole in a, and the universal relation between these two regions can be tested. Finally, much larger values of scattering length will be accessible, allowing to probe Efimov physics much deeper in the universal regime.

Methods

Preparation and detection

Our ultracold atom-dimer mixture is trapped in a crossed-beam optical dipole trap generated by two 1,064-nm laser beams with waists of about 250 μm and 36 μm [4]. Since atoms and dimers in general have different magnetic moments the application of a levitation field is not appropriate and a sufficiently high optical gradient in the vertical direction to hold the atoms and dimers against gravity is required. However, to obtain very low temperatures and not too high densities a tight trap is not advantageous. Here we use an adjustable elliptic trap potential with weak horizontal confinement and tight confinement in the vertical direction. The ellipticity is introduced by a rapid spatial oscillation of the 36-μm waist beam in the horizontal plane with the use of an acousto-optic modulator, creating a time-averaged optical potential. The final temperature of the atomic and molecular sample can be set by varying the ellipticity and the laser power of the laser beam in the final trap configuration. For the lowest temperature samples, the final time-averaged elliptic potential is characterized by trap frequencies of 10 Hz and 20 Hz in the horizontal plane, and 80 Hz in the vertical direction.

Dimer loss model

We measure the atom-dimer relaxation loss rate β by recording the time evolution of the dimer number N_{D} and atom number N_{A}. In a harmonic trap the atomic and molecular samples can be described by Gaussian density distributions, where the width depends on the trap frequencies, the temperature and the mass. Because the polarizability of the halo dimers is twice that of the atoms, the trap frequencies of the atoms and the dimers are the same. We find that the atomic and molecular samples have the same temperature [4]. The time-evolution of N_D can then be described by the following rate equation:

$$\dot{N}_{\mathrm{D}} = -\frac{8}{\sqrt{27}}\beta\bar{n}_{\mathrm{A}}N_{\mathrm{D}} - \alpha\bar{n}_{\mathrm{D}}N_{\mathrm{D}}, \tag{1}$$

with $\bar{n}_{\mathrm{A}} = [m\bar{\omega}^2/(4\pi k_{\mathrm{B}}T)]^{3/2}N_{\mathrm{A}}$ and $\bar{n}_{\mathrm{D}} = [m\bar{\omega}^2/(2\pi k_{\mathrm{B}}T)]^{3/2}N_{\mathrm{D}}$ the mean atomic and molecular density, respectively, m the atomic mass, $\bar{\omega}$ the geometric mean of the trap frequencies and T the temperature. Here loss of dimers due to dimer-dimer relaxation is also taken into account via the dimer-dimer relaxation loss rate coefficient α. Because of the unequal mass, the density distributions of the atomic and molecular samples are not the same. As a result, an effective atomic density experienced by the molecular cloud has to be considered, which is taken into account by the factor $\frac{8}{\sqrt{27}}$ in front of the atom-dimer loss term [23].

Our experiments are carried out in the regime in which $N_{\mathrm{A}} \gg N_{\mathrm{D}}$ and loss of atoms as a result of atom-dimer relaxation is negligible. Three-body recombination leads to atom loss on a much longer timescale compared to the molecular lifetime [14]. Therefore N_{A} can be taken as a constant and equation (1) has the following solution:

$$N_{\mathrm{D}}(t) = \frac{bN_{\mathrm{A}}N_{\mathrm{D},0}}{(bN_{\mathrm{A}} + aN_{\mathrm{D},0})e^{bN_{\mathrm{A}}t} - aN_{\mathrm{D},0}}, \tag{2}$$

where $N_{\mathrm{D},0} \equiv N_{\mathrm{D}}(t = 0)$, $b \equiv \frac{8}{\sqrt{27}}\beta[m\bar{\omega}^2/(4\pi k_{\mathrm{B}}T)]^{3/2}$ and $a \equiv \alpha[m\bar{\omega}^2/(2\pi k_{\mathrm{B}}T)]^{3/2}$. If $\beta N_{\mathrm{A}} \gg \alpha N_{\mathrm{D}}$, i.e. dimer-dimer relaxation loss is negligible compared to atom-dimer relaxation loss, equation (2) simplifies to

$$N_{\mathrm{D}}(t) = N_{\mathrm{D},0}e^{-bN_{\mathrm{A}}t}, \tag{3}$$

and N_{D} shows an exponential decay with a $1/e$ lifetime of $(bN_{\mathrm{A}})^{-1}$. In our experiments dimer-dimer relaxation loss can be neglected for $B > 20\,\mathrm{G}$ and equation (3) is fitted to the

data. For $B < 20\,\mathrm{G}$ β is much smaller than α [4] and the application of equation (2) is required, taking α from independent loss measurements of a pure dimer sample [4].

For each measurement of β the trap frequencies and the temperature are determined by sloshing mode and time-of-flight measurements, respectively. The error bars on β contain the uncertainties of these trap frequencies and temperature measurements.

Acknowledgements

We thank T. Köhler, B. Esry and P. Massignan for many fruitful discussions. We acknowledge support by the Austrian Science Fund (FWF) within SFB 15 (project part 16). S. K. is supported within the Marie Curie Intra-European Program of the European Commission. F. F. is supported within the Lise Meitner program of the FWF.

Competing financial interests

The authors declare no competing financial interests.

---

[1] Kraemer, T. *et al.* Evidence for Efimov Quantum States in an Ultracold Gas of Cesium Atoms. *Nature* **440**, 315 (2006).

[2] Braaten, E. & Hammer, H.-W. Universality in Few-Body Systems with Large Scattering Length. *Phys. Rep.* **428**, 259 (2006).

[3] Efimov, V. Energy Levels Arising from Resonant Two-Body Forces in a Three-Body System. *Phys. Lett. B* **33**, 563 (1970).

[4] Ferlaino, F. *et al.* Collisions between Tunable Halo Dimers: Exploring an Elementary Four-Body Process with Identical Bosons. *Phys. Rev. Lett.* **101**, 023201 (2008).

[5] Efimov, V. Low-Energy Properties of Three Resonantly Interacting Particles. *Sov. J. Nucl. Phys.* **29**, 546 (1979).

[6] Nielsen, E., Suno, H. & Esry, B. D. Efimov resonances in atom-diatom scattering. *Phys. Rev. A* **66**, 012705 (2002).

[7] Braaten, E. & Hammer, H.-W. Resonant dimer relaxation in cold atoms with a large scattering length. *Phys. Rev. A* **75**, 052710 (2007).

[8] Tiesinga, E., Verhaar, B. J. & Stoof, H. T. C. Threshold and resonance phenomena in ultracold ground-state collisions. *Phys. Rev. A* **47**, 4114 (1993).

[9] Inouye, S. *et al.* Observation of Feshbach Resonances in a Bose-Einstein Condensate. *Nature* **392**, 151 (1998).

[10] Courteille, Ph., Freeland, R. S., Heinzen, D. J., van Abeelen, F. A. & Verhaar, B. J. Observation of a Feshbach Resonance in Cold Atom Scattering. *Phys. Rev. Lett.* **81**, 69 (1998).

[11] Jensen, A. S., Riisager, K., Fedorov, D. V. & Garrido, E. Structure and Reactions of Quantum Halos. *Rev. Mod. Phys.* **76**, 215 (2004).

[12] Köhler, T., Góral, K. & Julienne, P. S. Production of cold molecules via magnetically tunable Feshbach resonances. *Rev. Mod. Phys.* **78**, 1311 (2006).

[13] Chin, C. *et al.* Precision Feshbach spectroscopy of ultracold Cs_2. *Phys. Rev. A* **70**, 032701 (2004).

[14] Weber, T., Herbig, J., Mark, M., Nägerl, H.-C. & Grimm, R. Three-body Recombination at Large Scattering Lengths in an Ultracold Atomic Gas. *Phys. Rev. Lett.* **91**, 123201 (2003).

[15] Mark, M. *et al.* Spectroscopy of ultracold trapped cesium Feshbach molecules. *Phys. Rev. A* **76**, 042514 (2007).

[16] Lee, M. D., Köhler, T. & Julienne, P. S. Excited Thomas-Efimov levels in ultracold gases. *Phys. Rev. A* **76**, 012720 (2007).

[17] Guéry-Odelin, D., Söding, J., Desbiolles, P. & Dalibard, J. Is Bose-Einstein condensation of atomic cesium possible? *Europhys. Lett* **44**, 25 (1998).

[18] Köhler, T. private communication (2007).

[19] Esry, B. D. private communication (2007).

[20] Massignan, P. & Stoof, H. T. C. Efimov states near a Feshbach resonance. Preprint at (http://arXiv:cond-mat/0702462v3) (2008).

[21] Wynar, R., Freeland, R. S., Han, D. J., Ryu, C. & Heinzen, D. J. Molecules in a Bose-Einstein Condensate. *Science* **287**, 1016 (2000).

[22] Mukaiyama, T., Abo-Shaeer, J. R., Xu, K., Chin, J. K. & Ketterle, W. Dissociation and Decay of Ultracold Sodium Molecules. *Phys. Rev. Lett.* **92**, 180402 (2004).

[23] Staanum, P., Kraft, S. D., Lange, J., Wester, R. & Weidemüller, M. Experimental Investigation of Ultracold Atom-Molecule Collisions. *Phys. Rev. Lett.* **96**, 023201 (2006).

[24] Zahzam, N., Vogt, T., Mudrich, M., Comparat, D. & Pillet, P. Atom-Molecule Collisions in

an Optically Trapped Gas. *Phys. Rev. Lett.* **96**, 023202 (2006).

[25] Syassen, N., Volz, T., Teichmann, S., Dürr, S. & Rempe, G. Collisional decay of ^{87}Rb Feshbach molecules at 1005.8 G. *Phys. Rev. A* **74**, 062706 (2006).

[26] Hudson, E. R., Gilfoy, N. B., Kotochigova S., Sage, J. M. & DeMille, D. Inelastic Collisions of Ultracold Heteronuclear Molecules in an Optical Trap. *Phys. Rev. Lett.* **100**, 203201 (2008).

[27] Ultracold Fermi Gases, Proceedings of the International School of Physics "Enrico Fermi", Course CLXIV, Varenna, 20 - 30 June 2006, edited by M. Inguscio, W. Ketterle, and C. Salomon (IOS Press, Amsterdam, 2008).

[28] Zirbel, J. J. *et al.* Collisional Stability of Fermionic Feshbach Molecules. *Phys. Rev. Lett.* **100**, 143201 (2008).

[29] Herbig, J. *et al.* Preparation of a Pure Molecular Quantum Gas. *Science* **301**, 1510 (2003).

[30] D'Incao, J. P. & Esry, B. D. Issues impacting the observation of Efimov physics in ultracold quantum gases. Preprint at (http://arXiv:cond-mat/0703269v1) (2007).

[31] Hammer, H.-W., Lähde, T. A. & Platter L. Effective-range corrections to three-body recombination for atoms with large scattering length. *Phys. Rev. A* **75**, 032715 (2007).

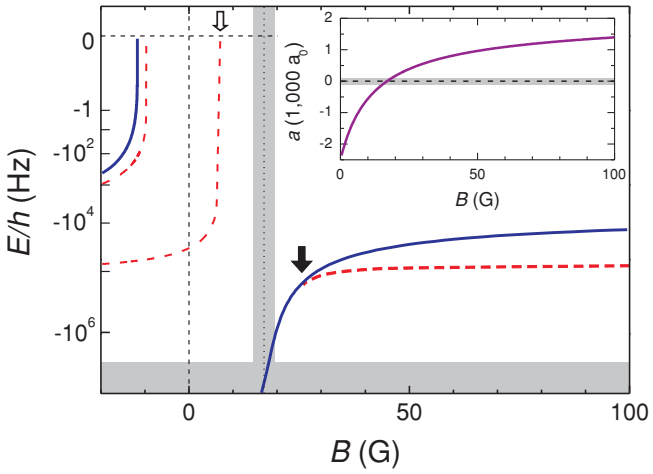

FIG. 1: **Three-body spectrum of caesium.** The energies E of the atom-dimer thresholds (blue solid curves) are shown as function of the magnetic field B. The red dashed lines illustrate Efimov-like trimer states, for which the energy dependence is not precisely known. The giant three-body loss resonance found at 7.5 G [1] has pinpointed the intersection of an Efimov state with the three-atom threshold (open arrow). The intersection of an Efimov state with an atom-dimer threshold (filled arrow) leads to a resonance in atom-dimer relaxation. Zero energy corresponds to three atoms in the lowest spin state, labeled by the total spin quantum number $F = 3$ and its projection $m_F = 3$. The inset shows the scattering length a as a function of the magnetic field B. The grey areas represent the non-universal regions, where $|a| < r_{\mathrm{vdW}} = 100\, a_0$ or $E_b > E_{\mathrm{vdW}} = h \times 2.7$ MHz.

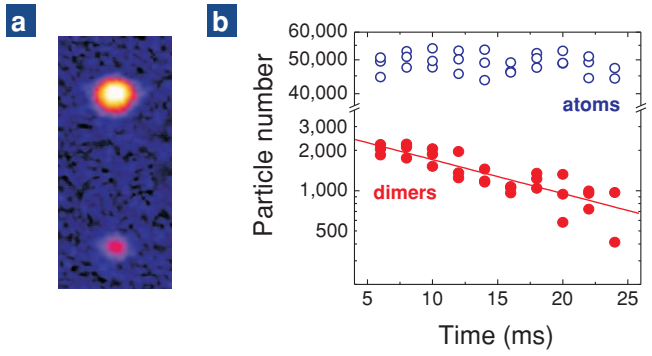

FIG. 2: **Measuring the atom-dimer relaxation loss rate. a,** Absorption image of the atom-dimer mixture after release from the trap and Stern-Gerlach separation. **b,** Time evolution of the number of atoms and dimers at 35 G. Here the loss of dimers can be fitted with an exponential decay curve with a $1/e$ lifetime proportional to β^{-1}, as the atom number greatly exceeds the dimer number and loss due to the dimer-dimer relaxation can be neglected (see Methods).

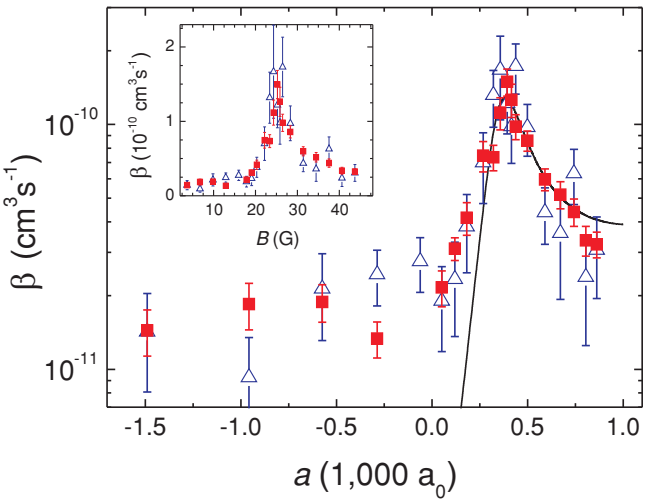

FIG. 3: **Loss resonance in atom-dimer relaxation.** The loss rate coefficient β for atom-dimer relaxation is shown as a function of the scattering length a (main figure) and the magnetic field B (inset); measurements are taken at temperatures of 40(10) nK (blue open triangles) and 170(20) nK (red closed squares). The solid curve is a fit of an analytic model from effective field theory (see text) to the data for $a > r_{\rm vdW} = 100\, a_0$.